International Research Journal of Engineering and Technology (IRJET) e-ISSN: 2395 -0056
Volume: 02 Issue: 09 | Dec-2015 www.irjet.net p-ISSN: 2395-0072

Dynamic Approach of MPPT for PV device by using Adaptive Control and fuzzy controller

Sasidhar sannidhi[1], Purushottam[2]

[1] *PG Scholar, Department of EEE, JNTU Anantapur, Andhra Pradesh, India*

[2] *PG Scholar, Department of EEE, JNTU Anantapur, Andhra Pradesh, India*

Abstract - ***In the solar systems to make as large power generation with good efficiency, it is important to locate the peak point (MPP) in real time. The characteristics of I-V curve in the solar array are non-linear, and the MPP may vary with the change of irradiation according to the nature. For the maximum power point tracking control is expected to obtain MPP without concern for both device and atmospheric conditions. An adaptive control technique is designed to construct the seeking algorithm operate to system states to the desired set points that maximize value of objective function. This dynamic technique includes (i) state space model of PV-buck system is obtained from approximate model based average system (ii) radial basis function based neural network used to approximate the non-linear(I-V) curve (iii) Lyapunov based adaptive learning control technique is applied to guarantee the convergence of overall system output. In this paper fuzzy controller is also applied to get the MPP of pv device The performance of adaptive control and fuzzy controller is verified with simulation results.***

Key Words: *AESC, model based average system, maximum power point control, radial basis function, Lyapunov based adaptive control, fuzzy controller.*

1. INTRODUCTION

In the recent years solar energy became one of the significant source of electrical energy because of its clean nature and renewable and another factor is its huge availability. But it has one disadvantage is the cost of pv device is more. So the cost of power generation is high in order to decrease the cost of power generation we have to operate pv device at high efficiency i.e. we have to operate pv device at maximum power point (MPP) position, but because of non linear characteristics of pv device it is difficult to find MPP point. There are two types of MPPT techniques static and dynamic optimization techniques. Where perturbation and observation (10), incremental inductance (5), hill climbing methods (11) are under the category of static methods. Static methods have low convergence and have a great effect of environment, to improve the transient response we follow dynamic methods (12)-(15). In this extremum seeking control (16)-(18) has better performance under variable environment conditions.

Apart from advantage of ESC it has some limitations because it is valid only neighborhood of equilibrium point. The stability and performance issues are based on the assumption of functional form of performance map. This ESC has the low convergence due to some limitations in loop gain by the stepper side. For this reason an alternate method was chosen i.e., adaptive control. The Adaptive controller is designed based on the knowledge of the system model structure and certain objective function that is defined based on measurable variables [20]. A parameter learning law is used for the unknown nonlinear relationship between states, and to ensure the convergence of the system a Lyapunov technique is used. The scheme searches for the both actual parameters and optimal inputs simultaneously. In particular, the PV output power is the product of the terminal voltage and current, thus the nonlinear characteristics of I(V) hinged by the objective function.

The radial basis function (RBF) neural network is used as the assumed functional for the Adaptive control (AESC) design [21].Similar to [21], the unknown *I (V)* characteristics approximated by Adopting Gaussian RBF kernel. The convergence of overall system output to an adjustable by applying a Lyapunov-based adaptive control technique approximation error-dependent neighbourhood of the optimum.

2. SOLAR SYSTEM MODEL

Two kinds of PV models are used in this brief for different purposes. First, a virtual plant built by the detailed physical based model for simulation. Then, a state-space model is obtained based on an approximate PV model for

PV-buck system, which is intended for adaptive controller design.

A. *physical modeling of solar PV for simulation:*

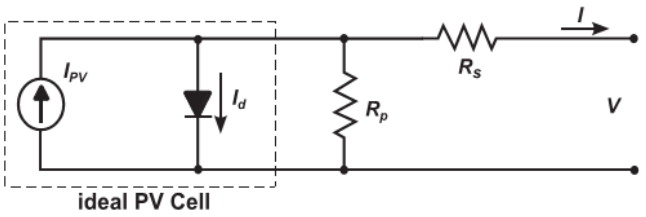

Fig 1: PV cell equivalent circuit

Its I–V relation can be modeled as,

$$I = I_{PV} - I_O\left[\exp\left(\frac{V+R_S}{V_{ta}}\right) - 1\right] - \frac{V+R_S I}{R_P} \qquad (1)$$

Where, V and I are the output voltage and current respectively. IPV is light generated current that is proportional to the irradiance, I0 is reverse saturation (or leakage) current of the diode.

$$V_t = \frac{N_S K T}{q}$$

Vt is thermal voltage of the array, Ns is number of cells connected in series, q is electron charge with the value of 1.60217646 ×10−19C, k =1.3806503 ×10−23J/K where k-Boltzmann constant, a is ideality factor, and Np is number of parallel connections of cells. Rs and Rp are the equivalent series and shunt resistance of the array.

$$I_{PV} = (I_{PV,n} + K_I \Delta T)\frac{G}{G_n} \qquad (2)$$

IPV is also to be influenced by the temperature [3] Where IPV,n is the light generated current at nominal conditions (25 °C and 1000 W/m2), and ΔT = T × Tn. T and Tn are the actual and nominal temperatures, respectively. The actual and nominal irradiance rates on the device are G and Gn, respectively. KI is the short circuit temperature coefficient. The diode saturation current I0 can be shown below [3]

$$I_O = I_{O,n}\left(\frac{T_n}{T}\right)^3 \exp\left[\frac{qE_g}{ak}\left(\frac{1}{T_n} - \frac{1}{T}\right)\right] \qquad (3)$$

Where Eg is the band gap energy of the semiconductor and I0 ,n is the nominal saturation current.

The below figure 2 shows the I–V and P–V characteristics. The generated current is shown to increase with the irradiance level.

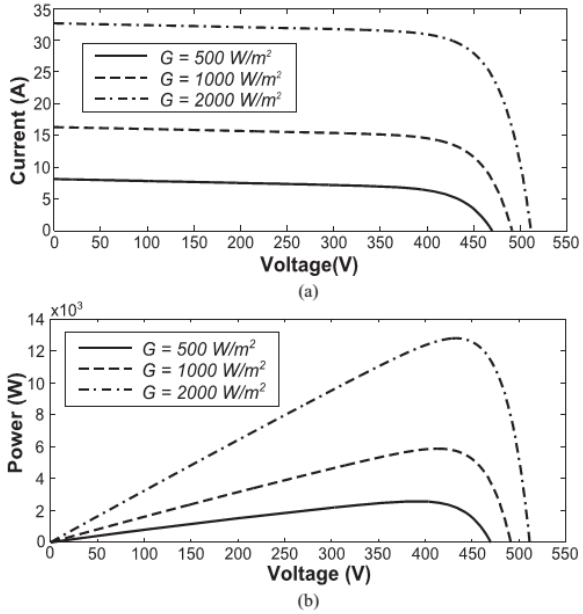

Fig 2: (a) I–V and (b) P–V curves at 25 °C under different irradiance rates.

Similarly, the I–V and P–V characteristics under nominal irradiance rate 1000W/m2 at different temperature values. With the increase of device temperature the power output is decreases. While the temperature change leads to changes of the MPP voltage then MPP voltage varies in all cases. So that adaptive MPPT control more beneficial in dealing with temperature changes.

The output of PV can be connected to battery or dc motor a dc–dc buck converter is needed for the conversion between different voltage levels. As this brief aims to value of an MPPT control algorithm of dc resistive load is adopted, as shown in fig.3

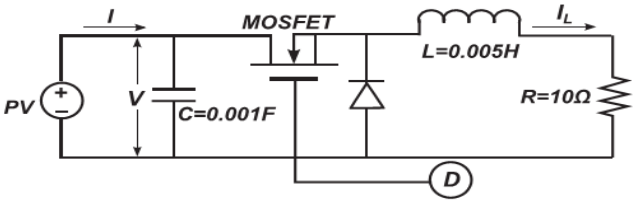

Fig 3: PV array with front-end buck converter

To achieve MPPT the duty ratio D of the pulse width modulator (PWM) is used to adjust the input voltage of the dc–dc converter and also the output of the PV array. The dc–dc converter are different types (A) buck, (B) boost, and (C) buck-boost types, is chosen in a case dependent fashion. In order to step down the voltage a buck type

converter is used, also shown in Fig.3. In this brief, we set the values of inductance L=5mH, the capacitor C=1 mF, and the resistive load R=10Ω.

B. Model-Based Averaged System:

From the fig 3, we can describe two sets of differential equations based on ON/OFF position of the MOSFET switch [13]. The state equations with switch on (State 1) is given as.

$$\frac{dV}{dt} = \frac{i(V)}{C} - \frac{i_L}{C} \qquad \dots(4a)$$

$$\frac{di_L}{dt} = \frac{V}{L} - \frac{i_L}{R} \qquad \dots(4b)$$

Where i(V) is the mapping between the output current and the terminal voltage of the PV array, and iL is the inductor current. If the switch is turn OFF (State 0), the equations become

$$\frac{dV}{dt} = \frac{i(V)}{C} \qquad \dots(5a)$$

$$\frac{di_L}{dt} = -\frac{i_L R}{L} \qquad \dots(5b)$$

From equation (4) and (5) we get unified system dynamics by averaging method

$$\frac{dV}{dt} = \frac{i(V)}{C} - \left(\frac{i_L}{C}\right)D \qquad \dots(6a)$$

$$\frac{di_L}{dt} = -\frac{i_L R}{L} + \left(\frac{V}{L}\right)D \qquad \dots(6b)$$

Where D is duty ratio it is defined as the portion of State 1 within a period of PWM operation. For the better approximation of non-linear i(V) in parameter updating, the ranges of V and iL

$$\frac{dp}{dt} = -\frac{R}{L}p + \frac{k_{g1}}{L}q.v$$

$$\frac{dq}{dt} = \frac{k_{g2}}{k_{g1}C}\mu(q) - \frac{1}{k_{g1}C}p.v$$

$$y = k_{g1}k_{g2}\mu(q).q \qquad (7)$$

Where p is the $i_L \in [0,+\infty)$ is the inductance current, q is the $V/k_{g1} \in [0, V_M/k_{g1}]$ is the scaled PV terminal voltage with $kg_1=100$, and V_M is the maximum voltage of the PV system. $\mu=i(V)/k_{g2} \in [0,I_M/k_{g2}]$ with $k_{g2}=10$, I_M is the maximum current, y(=P)=iV is the power output, and v= D∈ [0, 1] is the control input to be designed for MPPT control. The objective of the AESC design is to search for the maximum power output y.

3. MPPT design of PV device using AESC and Fuzzy logic controller

3. A. AESC DESIGN FOR MPPT PROBLEM:

The Adaptive controller aims to find the unknown operating set-points that optimize the desired objective function [19]. Consider the normalized system dynamics [21].

$$\dot{p} = f(p, \mu(p), v) \qquad (8a)$$

and the objective function is

$$y = g(p, \mu(p)) \qquad (8b)$$

Where output y is assumed as indirect measureable. The structure information for f(p,μ(p),v) and g(p,μ(p)) are required for the Adaptive control design with the observable system states p∈ R n ,and the static nonlinearity may exist in the system is μ(p). The adaptive controller that can reach the optimum solution for objective function and convergence of parameters describe by using inverse optimal solution [21]. The unknown nonlinearity μ(p) can be approximated by the kernel functions, the RBF neural network was proposed to uniformly approximate the continuous nonlinearity μ(p) on a compact set [21]-[22].

$$\mu[p(t)] = w^{*T}Q[p(t)] + \mu_l(t) \qquad (9a)$$

Where μl(t) is the approximation error. The radial basis function vector is given by

$$Q[p(t)] = [q_1[p(t)], q_2[p(t)] \dots . q_l[p(t)]] \qquad (9b)$$

The ideal weight W∗ is obtained by

$$W^* = arg\ \min_{w\in\Omega}\{\sup\ |W^TQ(p) - \mu(p)| \qquad (10)$$

Where Ωw={W|IIWII ≤wm}. w_m is a positive constant

An adaptive learning technique used projection algorithm for online estimation of unknown parameters. To ensure the convergence of the system a Lyapunov-based controller is used. For problem formulation and controller design procedure are described as follows. The equilibrium or steady-state output power is

$$y_e = k_{g1}k_{g2}\mu(q_e)q_e \qquad (11a)$$

Substituting (9a) into (11a) yields

$$y_e = k_{g1}k_{g2}\left(W^{*T}Q(q_e) + \mu_l(t)\right)q_e \qquad (11b)$$

In (11a), μ(q) represents the value of i(V)/k_{g2},whichis bounded and in the range of [0,I_M/k_2]. The term of $W^{*T}q(q)$ is bounded by construction. Thus, we can have the assumption $|\mu_l(t)| \leq \mu_l$ over a compact set with constant $\mu_l>0$. Let the first-and second-order derivatives of (11) yield

$$\frac{dy_e}{dq_e} = k_{g1}k_{g2}W^{*T}[dQ(q_e) + Q(q_e)] + k_{g1}k_{g2}\mu_{l(t)} \quad 12a$$

$$\frac{d^2}{dy_e^2}y_e = k_{g1}k_{g2}W^{*T}[d^2Q(q_e) + 2dQ(q_e)] \quad 12b$$

Where Q=∂Q/∂q and d2Q = ∂2Q/∂q2. The basis function vector Q(q) is given by

$$Q(q) = [b_1(s)b_2(s)\ldots. \quad b_l(s)] \qquad (13a)$$

and Gaussian kernels are adopted

$$b_i(q) = \exp\left[\frac{-(q-\Phi_i)^T(q-\Phi_i)}{\sigma_i^2}\right] \qquad (13b)$$

Where φi and σi are the center and the width of the Gaussian function, respectively. Basis function derived as

$$\frac{dQ_i}{dq} = -2\frac{(q-\Phi_i)}{\sigma_i^2}\exp\left[\frac{-(q-\Phi_i)^T(q-\Phi_i)}{\sigma_i^2}\right] \qquad (14a)$$

$$\frac{d^2Q_i}{dq^2} = \left(-2\frac{1}{\sigma^2} + 4\frac{(q-\Phi_i)^2}{\sigma^4}\right)\exp\left[\frac{-(q-\Phi_i)^T(q-\Phi_i)}{\sigma_i^2}\right] \qquad (14b)$$

The objective of MPPT problem is to design a control law and parameter estimation law such that the maximum steady-state power output y* can be found, and the weight W*can be obtained to achieve the ideal approximation [1]. Substitute of (9a), (7a) and (7b) become

$$\dot{p} = -\frac{R}{L}p + \frac{k_{g1}}{L}q.v \qquad (15a)$$

$$\dot{q} = \frac{k_{g2}}{k_{g1}C}\left[W^{*T}Q(q) + \mu_l(t)\right] - \frac{1}{k_{g1}}p.v \qquad (15b)$$

Let Wˆ is the estimate of the true weights W*. Let qˆ and pˆ are the predictions of q and p, respectively. The dynamics of these predicted states can be derived as

$$\dot{\hat{p}} = -\frac{R}{L}p + \frac{k_{g1}}{L}q.v + k_{gx} + c_1(t)^T\dot{\hat{W}} \qquad (16a)$$

$$\dot{\hat{q}} = \frac{k_{g2}}{k_{g1}C}\left[W^{*T}Q(q) + \mu_l(t)\right] - \frac{1}{k_{g1}}p.v - k_{gq}e_q - c_2(t)^T\dot{\hat{W}} \quad (16b)$$

Where k_p, k_q, $c_1(t)$,and$c_2(t)$ need to be designed. The dynamics for the state estimation errors e_p =p− pˆ and e_q =q−qˆ as

$$\dot{e_p} = k_{gp}e_p - c_1(t)^T\dot{\tilde{W}} \qquad (17a)$$

$$\dot{e}_q = \frac{k_{g2}}{k_{g1}C}\left[W^{*T}Q(q) + \mu_l(t)\right] - k_{gq}e_s - c_2(t)^T\dot{\tilde{W}}$$

(17b)

With W˜=W*−Wˆ difference between estimated gradient and 0 is called gradient tracking error.

$$z = k_{g1}k_{g2}\dot{W}^T[dQ(q) + Q(q)] \qquad (18)$$

To operate the parameter and state estimation, a dither signal d(t) is added

$$z_q = \dot{W}^T[dQ(q) + Q(q)] - d(t) \qquad (19)$$

For which $k_{g1}k_{g2}>0$ are removed for simplicity tracking error dynamics are,

$$\dot{z}_e = \dot{\tilde{W}}^T[dQ(q)\dot{q} + Q(q)] + \dot{\tilde{W}}^T[d^2Q(q)\dot{q}\dot{q} + 2dQ(q)\dot{q}] - \dot{d}(t) \quad 20$$

Let

$$L1 = dQ(q)q + Q(q)$$
$$L2 = d^2Q(q)q + 2dQ(q)$$

Define the variables

$$\beta_1 = e_p - c_1(t)^T\tilde{W} \qquad (21a)$$

$$\beta_2 = e_q - c_2(t)^T\tilde{W} \qquad (21b)$$

$$\beta_3 = z_q - c_3(t)^T\tilde{W} \qquad (21c)$$

Now consider the Lyapunov function

$$V = \frac{1}{2}\beta^T\beta = \frac{1}{2}\beta_1^2 + \beta_2^2 + \beta_3^2\beta_1^2 \qquad (22)$$

From the derivative $\dot{V}$, dither signal as

$$d(\dot{t}) = c_3(t)^T\hat{\hat{W}} + \hat{\hat{W}}^T L1 - k_{gd}d(t) - \hat{W}^T L2\, a(t) \quad (23)$$

With k_{gd}>0 and external signal a(t)[1]. Then the control law is

$$v = \frac{k_{g1}}{C}\left[\frac{k_{g2}}{k_{g1}C}\hat{W}^T Q(q) - a(t) + \left(\frac{k_{gd}}{\hat{W}^T L2}\right)d(t) + \left(\frac{k_z}{\hat{W}^T L2}\right)z_q\right]$$

(24)

3.B. MPPT of PV device by using fuzzy logic controller:

The control algorithm of a process that is based on fuzzy logic or a fuzzy inference system is defined as fuzzy controller. One of the most advantages with fuzzy logic controller is that, this controller does not need any mathematical model for the plant, like any other conventional controllers as exists. Fuzzy logic controller is also nonlinear control, which gives robust performance for linear as well as nonlinear plants, with input parameter variation. Recently fuzzy logic controllers have been introduced in the tracking of the MPP in PV systems. They have the advantage to be robust and relatively simple to design as they do not require the knowledge of the exact model. They do require in the other hand the complete knowledge of the operation of the PV system by the designer.

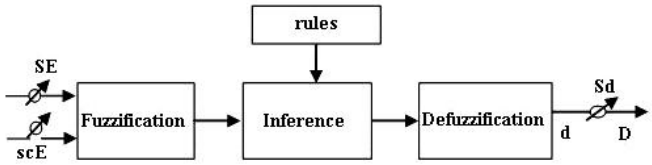

Fig 4: General diagram of a fuzzy controller

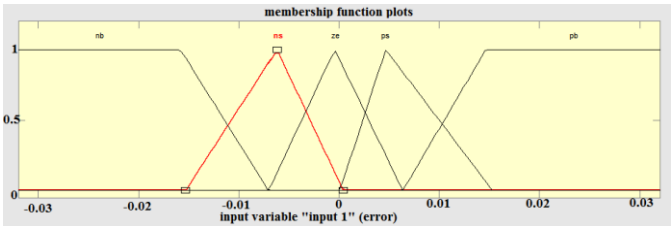

Fig 5 a: Membership function of input 1 (error =Δp/Δv)

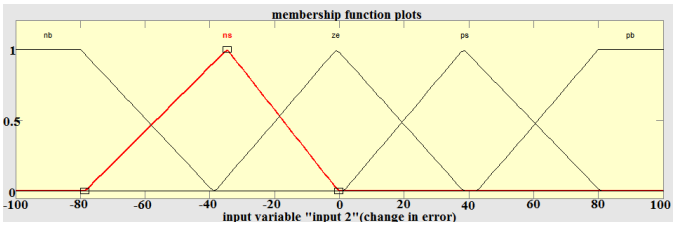

Fig 5 b: Membership function of input 2 (change in error)

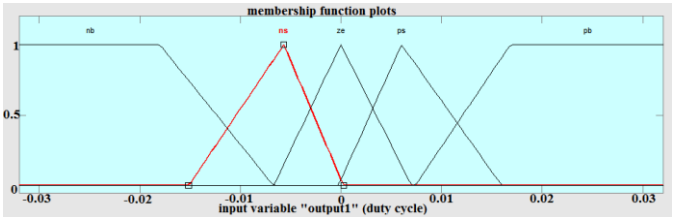

Fig 5 c: Membership function of output (duty ratio)

Table 1: Fuzzy rule table

And logic	NB	NS	ZE	PS	PB
NB	ZE	ZE	PB	PB	PB
NS	ZE	ZE	PS	PS	PS
ZE	PS	ZE	ZE	ZE	NS
PS	NS	NS	NS	ZE	ZE
PB	NB	NB	NB	ZE	ZE

The proposed fuzzy logic MPPT controller has two inputs and one output. Inputs are error and change in error and the output is duty cycle.

4. SIMULATION RESULTS

The simulation study is performed on the solar system with dc-dc buck converter described in Section 2, and the adaptive controller designed in Section 3. The simulation platform is Simulink 7.3 Sim Power Systems with MATLAB R2009a. The initial condition of the system and estimated values was set to iL(0)=0.1A V(0)=0.1V, p^(0)=0.1, q^(0)=0.1. The design parameters in the adaptive controller (24) and the parameter update law (27) are chosen as γw=100, kgd=0.1, kz0=1, kp0=1000, kq0=1, kg3=1 and kg4=0.1. A five-term RBF is selected with centers and width as

$$\Phi_i = 0.6+4.8(i-1)/4 \; _i = 0.6,\ i=1,2.....10.$$

To cover the range of [0, 6] the initial conditions for the $W^{\wedge}{}_i$=0.1, i=1,2…5, parameter update weights are set as $W^{\wedge}{}_i$ (0)=0.1, i =1, 2,...,5. The external signal a(t) is designed as

$$a(t)=10-4.\sum\omega_i\,[A_{1i}\sin(\omega_i t)+A_{2i}\cos(\omega_i t)]$$

A_{1i} and A_{2i} are randomly chosen from a unit normal distribution. The frequencies are chosen as $\omega_i=10^3[1+(i-1)10/9]$, i=1,2,3....10, $c_1(t)$, $c_2(t)$,and $c_3(t)$ are initialized as zero vectors, while for the dither signal d(t), d(0)=0.

To evaluate the performance of the Adaptive MPPT scheme, three different scenarios are studied. First, simulation is performed with a step change of irradiance rate from 1000 W/m² (0 ~0.1 s) to 300 W/m² (0.1 ~0.2 s). Below figure shows searched PV power output performance [1]. The steady-state power outputs of the PV array are 5830 and 1320 W, respectively, with the theoretical optima of 5884 and 1329 W, respectively. Notice that the PV array power output with former control input (duty ratio) is 750W. A 560W difference is gained by adaptive MPPT method with the 1% setting time of about 0.024 sec.

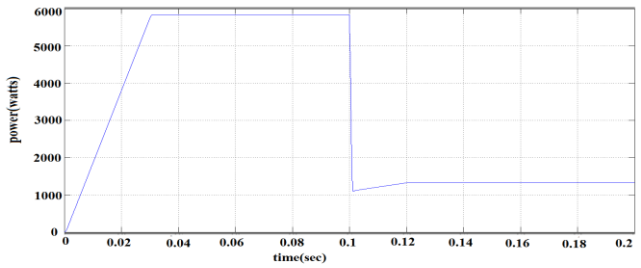

Fig 6: power output under a step change of irradiance rate from 1200 to 300 W/m2

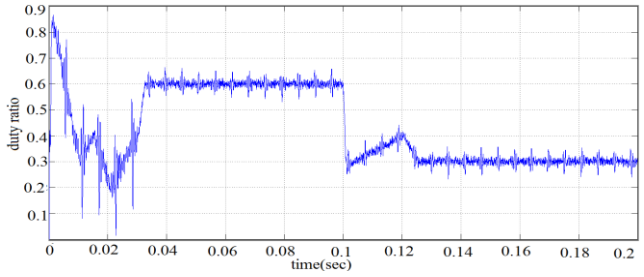

Fig 7: Duty ratio for dynamic MPPT under a step change of irradiance rate from 1000 to 300 W/m2.

Observable variation of the steady-state output is due to the fluctuation in a(t),which sustains the persistence excitation condition for parameter estimation. For a ramp change of temperature from 298 K (0~0.1s) down to 290 K (0.2~0.3s) with a 0.1sec ramp period (0.1~0.2 s). The amplitude of a(t) is reduced due to the smaller change of temperature comparing to the irradiance change. The below figure shows the PV power output by the MPPT. The steady-state power outputs of the PV array are 5859 and 6049 W, respectively, with the theoretical optima of 5884 and 6052 W.

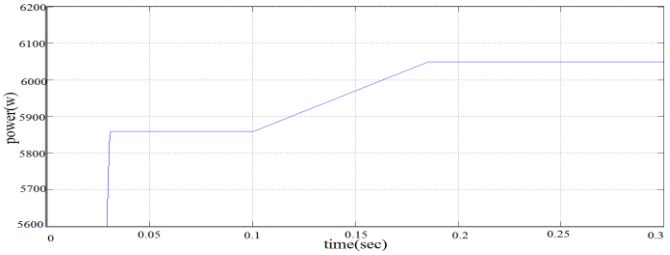

Fig 8 (a): power output under ramp change of temperature from 25°C17°C

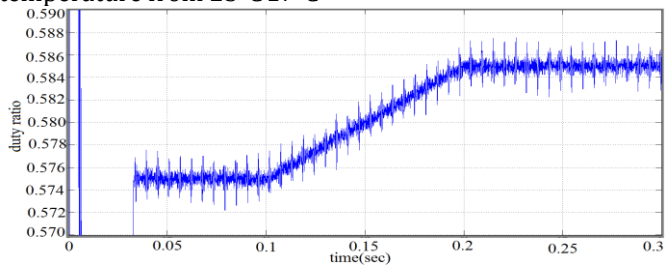

Fig 8 (b): Duty ratio under a ramp change of temperature from 25 °C to 17°C.

Finally, the AESC is simulated with a combined change of irradiance rate and temperature as shown in below figure.

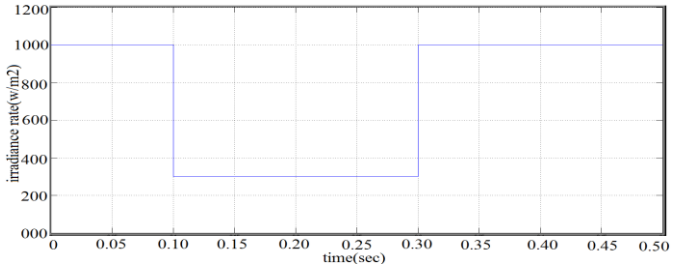

Fig 9: change in irradiation rate

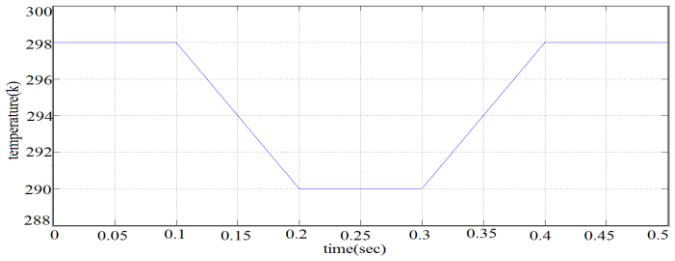

Fig 10: Change in temperature

The below Figure shows the AESC searched PV power output performance under Combined change of irradiance rate and temperature.

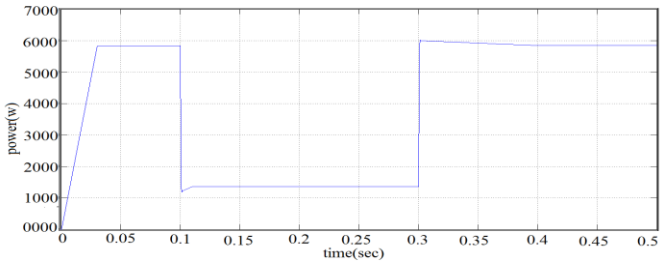

Fig 11: PV power output for AESC MPPT under a combined change of irradiance rate and temperature.

The steady-state power outputs of the PV array are 5838, 1365, and 5841 W, respectively, with theoretical optima of 5884, 1366, and 5884 W, respectively.

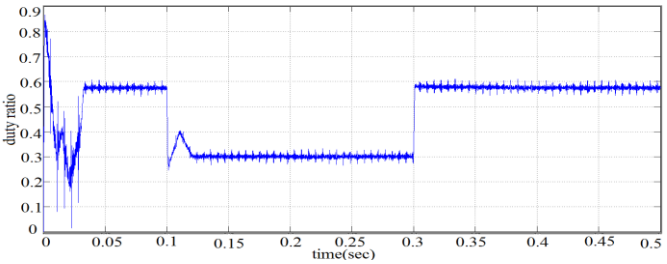

Fig 12: Duty ratio profile for AESC MPPT under a combined change of irradiance rate and temperature.

4.B. Fuzzy logic controller simulation results:

The simulation study is performed on the solar system by using fuzzy logic the fuzzy inference is carried out by using Mamdani's method and fuzzy logic controller for MPPT problem is designed. The following figures shows output waveforms.

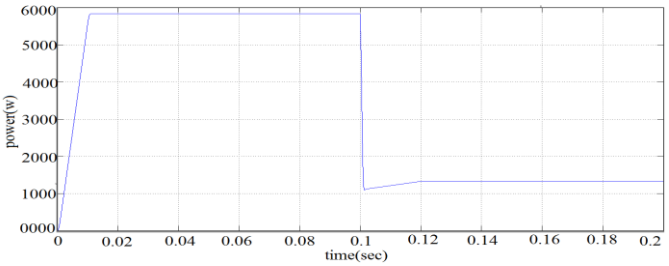

Fig 13 (a): power output under a step change of irradiation

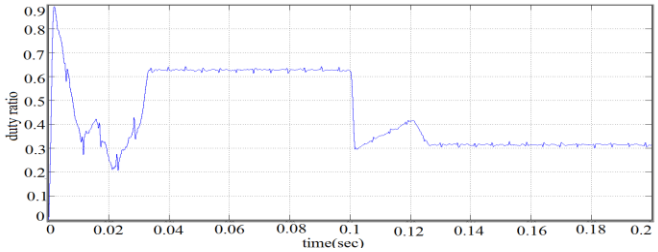

Fig 13 (b): under a step change of irradiance rate from 1200 to 300 W/m2

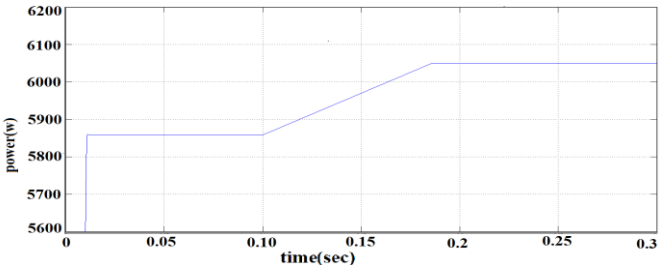

Fig 14 (a): power output under a ramp change of temperature

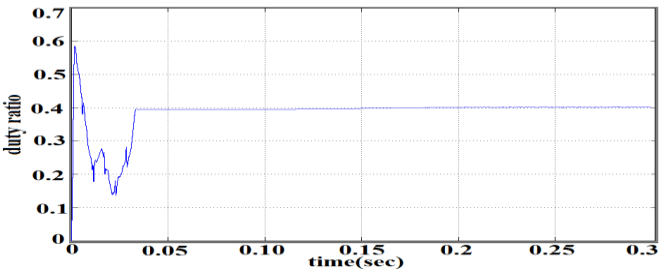

Fig 14(b): Duty ratio under a ramp change of temperature

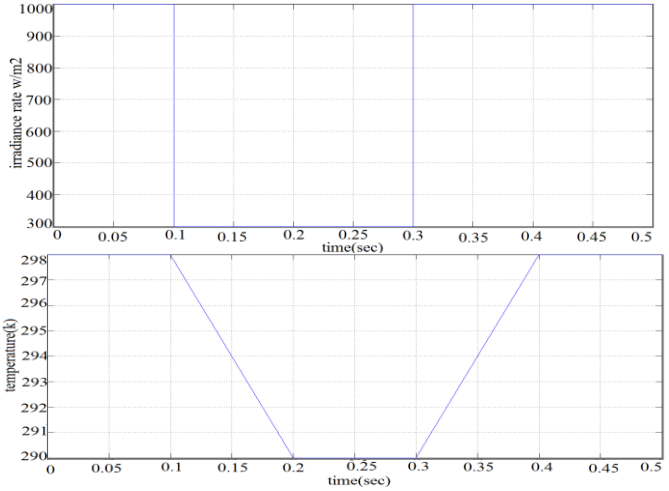

Fig 15: Combined change of both irradiation rate and temperature.

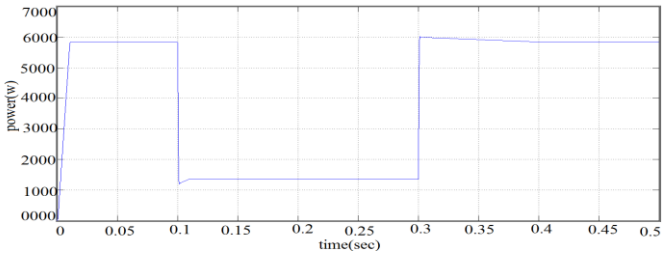

Fig 16: power output under the change of both temperature and irradiation

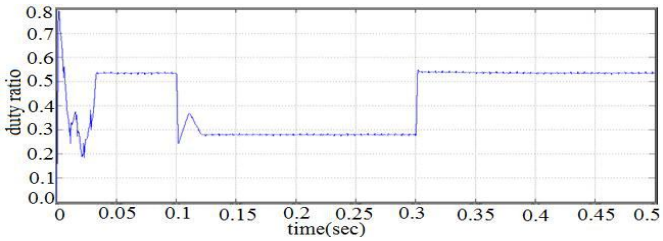

Fig 17: Duty ratio under the change of both temperature and irradiation is shown in above figure.

5. CONCLUSION

The operation of pv device at MPPT is necessary to achieve power generation at low cost. In this paper, two new methods of MPPT of pv device are introduced. These two models have same input i.e. irradiation and temperature The adaptive controller was applied to the solar MPPT problem, by utilizing RBF to approximate the unknown nonlinear I–V curve. The duty ratio for the buck converter is used to modulate the PV terminal voltage. From adaptive update law both MPP and RBF parameters were trained. And also fuzzy logic controller is designed for MPPT of pv device.

From the above simulation results, AESC Controller and fuzzy logic Controller have been compared using difference between the power outputs. As it is demonstrated fuzzy logic Controller has the better response than AESC controller. These two controllers had trained with full range optimal value of pv device input-output successfully. Thus it is clear that output power of pv device was nominal and obtained by using AECS controller. For this method a limitation is that more disturbances occur. Practically, both the approaches gave acceptable results. But consequently, considering the desired values in training, fuzzy logic controller gives output with fewer ripples.

REFERENCES

[1] Xiao lLi, and John E Seem "Maximum Power Point tracking control for Photovoltaic System Using Adaptive extremum control" IEEE Transs. Control System Technology, Nov 2013

[2] H. P. Desai and H. K. Patel, "Maximum Power Point Algorithm in PV Generation: An Overview," in *Power Electronics and Drive Systems* 2007, pp. 624-630.

[3] M. G. Villalva, J. R. Gazoli, and E. R. Filho, Comprehensive approach to modeling and simulation of photovoltaic arrays," *IEEE Trans. Power Electron.*, vol. 24, no. 5, pp. 1198–1208, May 2009.

[4] N. Femia, G. Petrone, G. Spagnuolo, and M. Vitelli, "Optimization of perturb and observe maximum power point tracking method," *IEEE Trans. Power Electron.*, vol. 20, no. 4, pp. 963–973, Jul. 2005.

[5] K. H. Hussein, I. Muta, T. Hoshino, and M. Osakada, "Maximum photovoltaic power tracking: An algorithm for rapidly changing atmospheric conditions," *IEE Proc.-Generat., Transmiss. Distrib.*, vol. 142, no. 1, pp. 59–64, Jan. 1995.

[6] P. Lei, Y. Li, and J. E. Seem, "Extremum seeking control based integration of MPPT and degradation detection for photovoltaic arrays," in *Proc. Amer. Control Conf.*, 2010, pp. 3536–3541.

[7] S. L. Brunton, C. W. Rowley, S. R. Kulkarni, and C. Clarkson, "Maximum power point tracking for photovoltaic optimization using ripple-based extremum seeking control," *IEEE Trans. Power Electron.*, vol. 25, no. 10, pp. 2531–2540, Oct. 2010.

[8] P. Lei, Y. Li, and J. E. Seem, "Sequential ESC-based global MPPT control for photovoltaic array with variable shading," *IEEE Trans.Sustain. Energy*, vol. 2, no. 3, pp. 348–358, Jul. 2011.

[9] S. J. Moura and Y. A. Chang, "Asymptotic convergence through Lyapunov-based switching in extremum seeking with application to photovoltaic systems," in *Proc. Amer. Control Conf.*, Baltimore, MD, 2010, pp. 3542–3548.

[10] S. J. Moura and Y. A. Chang, "Asymptotic convergence through Lyapunov-based switching in extremum seeking with application to photovoltaic systems," in *Proc. Amer. Control Conf.*, Baltimore, MD, 2010, pp. 3542–3548.

[11] E. Koutroulis, K. Kalaitzakis, and N. C. Voulgaris, "Development of a microcontroller-based, photovoltaic maximum power point tracking control system," *IEEE Trans. Power Electron.*, vol. 16, no. 1, pp. 46–54, Jan. 2001.

[12] B. M. Wilamowski and X. Li, "Fuzzy system based maximum power point tracking for PV system," in *Proc. IEEE 28th Annu. Conf. Ind.Electron. Soc.*, Mar. 2002, pp. 3280–3284.

[13] C.-C. Chu and C.-L. Chen, "Robust maximum power point tracking method for photovoltaic cells: A sliding mode control approach," *Solar Energy*, vol. 83, no. 8, pp. 1370–1378, 2009.

[14] T. Hiyama, S. Kouzuma, and T. Imakubo, "Identification of optimal operating point of PV modules using neural network for real time maximum power tracking control," *IEEE Trans. Energy Convers.*, vol. 10, no. 2, pp. 360–367, Jun. 1995

[15] R. Leyva, C. Alonso, I. Queinnec, A. Cid-Pastor, D. Lagrange, and L. Martinez-Salamero, "MPPT of photovoltaic systems using extremum seeking control," *IEEE Trans. Aerosp. Electron. Syst.*, vol. 42, no. 1, pp.249–258, Jan. 2006.

[16]Y. Tan, D. Nesic, and I. Mareels, "On the choice of dither in extremum seeking systems: A case study," *Automatica*, vol. 44, no. 5, pp. 1446–1450, 2008.

[17] Y. Tan, D. Nesic, I. M. Y. Mareels, and A. Astolfi, "On global extremum seeking in the presence of local extrema," *Automatica*, vol. 45, no. 1, pp. 245–251, 2009.

[18] D. Nešic, "Extremum seeking control: Convergence analysis," *Eur. J.Control*, vol. 15, nos. 3–4, pp. 331–347, 2009.

[19] M. Guay and T. Zhang, "Adaptive extremum

seeking control of nonlinear dynamic systems with parametric uncertainties," *Automatica*, vol. 39, no. 7, pp. 1283–1293, 2003.
[20] M. G. Villalva, J. R. Gazoli, and E. F. Ruppert, "Modeling and circuitbased simulation of photovoltaic arrays," *Brazilian J. Power Electron.* vol. 14, pp. 35–45, Aug. 2009.
[21] M. Guay, D. Dochain, and M. Perrier, "Adaptive extremum seeking control of continuous stirred tank bioreactors with unknown growth kinetics," *Automatica*, vol. 40, no. 5, pp. 881–888, 2004.

BIOGRAPHIES

SASIDHAR SANNIDHI received B-TECH. degree in electrical engineering from RGMCET NANDYAL, ANDHRA PRADESH, INDIA, in 2012. He is currently pursuing the M-TECH. degree in electrical engineering from J.N.T.U.A ANANTHAPUR, ANDHRA PRADESH

PURUSHOTTAM received B-TECH. degree in electrical engineering from SIET, PUTTUR, ANDHRA PRADESH, INDIA, in 2013. He is currently pursuing the M-TECH. degree in electrical engineering from J.N.T.U.A ANANTHAPUR, ANDHRA PRADESH